

GIANT FERROMAGNETIC HALL COEFFICIENT IN $\text{La}_{0.5}\text{Ca}_{0.5}\text{CoO}_3$

A. V. SAMOILOV,* N. - C. YEH,* and R. P. VASQUEZ#

*Department of Physics 114-36, California Institute of Technology, Pasadena, CA 91125

Center for Space -Microelectronics Technology, Jet Propulsion Laboratory, California Institute of Technology, Pasadena, CA 91109

ABSTRACT

We report the studies of the Hall effect and magnetic properties in $\text{La}_{0.5}\text{Ca}_{0.5}\text{CoO}_3$ thin films and ceramics. We use the local Hall probe and SQUID magnetometers to measure the magnetization M of the samples. Both below and above the Curie temperature, the Hall resistivity $\rho_{xy}(H)$ is shown to be proportional to $M(H)$ (H is the applied magnetic field). Thus, our results provide convincing evidence for the anomalous Hall effect in these cobaltites. The value of the anomalous Hall coefficient R_s in $\text{La}_{0.5}\text{Ca}_{0.5}\text{CoO}_3$ significantly exceeds those of other known single-phase ferromagnetic metals. We suggest that the coexistence of high- and low-spin configurations in the perovskite cobaltites, which gives rise to magnetic percolation behavior in $\text{La}_{1-x}\text{Ca}_x\text{CoO}_3$, may be responsible for the giant R_s .

INTRODUCTION

In magnetic metals, the Hall resistivity ρ_{xy} can be presented as a sum of the following two terms:

$$\rho_{xy} = R_0 B + R_s (\mu_0 M). \quad (1)$$

Here, B is the magnetic induction and M is the magnetization of the sample. The first term is due to the Lorentz force on the conduction electrons, and the second one is called the anomalous Hall resistance. R_0 and R_s are normal and anomalous Hall coefficients, respectively, and usually in ferromagnets $R_0 \ll R_s$.

The anomalous Hall effect arises if the scattering of the charge carriers is asymmetric with respect to the plane spanned by the electrical current and magnetization. The origin of this effect is believed¹ to be related to the spin-orbit interaction which can give rise to a left-right symmetry breaking in the scattering probability²⁻⁴. Although it has been noted in the early literature¹ that the theoretical value^{3,4} of R_s is small by two orders of magnitude to account for the experimental results in iron and nickel, this question concerning the absolute value of R_s has never been given appropriate attention. In this paper, we present results of the transport and magnetic measurements in a rare-earth cobaltite with the perovskite structure, $\text{La}_{0.5}\text{Ca}_{0.5}\text{CoO}_3$. We show that, to our knowledge, the value of R_s in this material not only is the largest value among ferromagnetic metals but also exceeds theoretical estimates by many orders of magnitude.

SPECIFIC FEATURES OF $\text{La}_{0.5}\text{Ca}_{0.5}\text{CoO}_3$

In the parent compound LaCoO_3 , the crystal-field splitting is larger than the exchange Hund's energy⁵. Therefore, at low temperatures, the trivalent Co ions have a low-spin $t_{2g}^6 e_g^0$ (with spin $S=0$) configuration (Co^{III} , see Fig. 1). The uniqueness of this system is that the

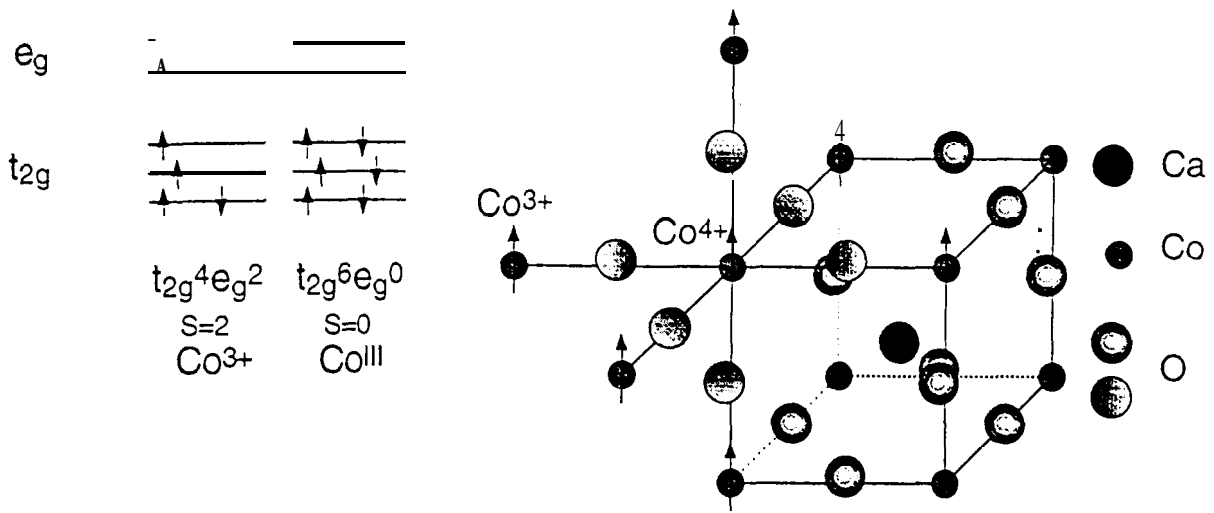


Fig. 1. Left panel: High-spin and low-spin configurations of trivalent Co ions. Right panel: $[\text{Co}^{IV}-6\text{Co}^{3+}]$ complex formed near dopant Ca atom.

balance between the crystal-field splitting and the Hund's energy is delicate and, correspondingly, the energy difference between these low-spin and the high-spin configurations is small (approximately 80 meV^5). Both increasing temperature and increasing doping of divalent ions to the rare-earth cation site can result in the stabilization of the high-spin states. In order to show how the substitution of divalent Ca for trivalent La gives rise to the augmenting population of the high-spin ($S=2$) $t_{2g}^4 e_g^2$ configuration Co^{3+} , we will use the explanation suggested by Senaris and Goodenough for a similar compound, $\text{La}_{1-x}\text{Sr}_x\text{CoO}_3^5$.

The substitution of divalent Ca results in the appearance of tetravalent Co^{IV} ($t_{2g}^5 e_g^0$) ions which polarize the oxygen p -electrons. This polarization towards Co^{IV} ions reduces the effect of the crystal field on the trivalent Co ions on the opposite side of the oxygen atoms (Fig. 1) and stabilizes the high-spin $t_{2g}^4 e_g^2$ configuration. As a result, magnetic clusters $[\text{Co}^{IV}-6\text{Co}^{3+}]$ are formed near each Ca atom.

With increasing doping level, the magnetic clusters reach a magnetic percolation threshold. Chemically-doped holes induce ferromagnetism via the so-called double-exchange interactions—s. $\text{La}_{1-x}\text{Sr}_x\text{CoO}_3$, is found to have metallic electrical conduction for $0.3 \leq x \leq 0.5$, with “hole-poor” lower-spin matrix interpenetrating the metallic “hole-rich” higher-spin regions⁵. In $\text{La}_{1-x}\text{Ca}_x\text{CoO}_3$ ferromagnetism is established approximately for the same values of x , with the Curie temperature $T_c = 150 \text{ K} - 185 \text{ K}^9$.

EXPERIMENTAL

The $\text{La}_{0.5}\text{Ca}_{0.5}\text{CoO}_3$ epitaxial films are grown by pulsed laser deposition using a stoichiometric target of $\text{La}_{0.5}\text{Ca}_{0.5}\text{CoO}_3$, in 100 mTorr of oxygen. The temperature of the LaAlO_3 substrates is 700°C . The growth is followed by annealing in 1 atm. oxygen at 900°C for two hours, and the epitaxy of the films is confirmed by x-ray rocking curves. The Hall effect is studied in two thin film samples $2 \text{ mm} \times 2 \text{ mm} \times 150 \text{ nm}$ (sample 1) and $5 \text{ mm} \times 5 \text{ mm} \times 300 \text{ nm}$ (sample 2) in size and in two ceramic oxygen-deficient samples, $5 \text{ mm} \times 3 \text{ mm} \times 1.9 \text{ mm}$ in size.

For the Hall measurements, we have deposited four gold pads on the corners of the film (or on the edges of the ceramic samples) and employed the van der Pauw method¹⁰ to measure both the Hall and longitudinal resistivities. We have performed measurements at 10-20 different values of electrical current in the range of 0 - $10 \mu\text{A}$ for the films and 0 - 20 mA for the ceramic samples at selected temperatures and magnetic fields to ensure linear

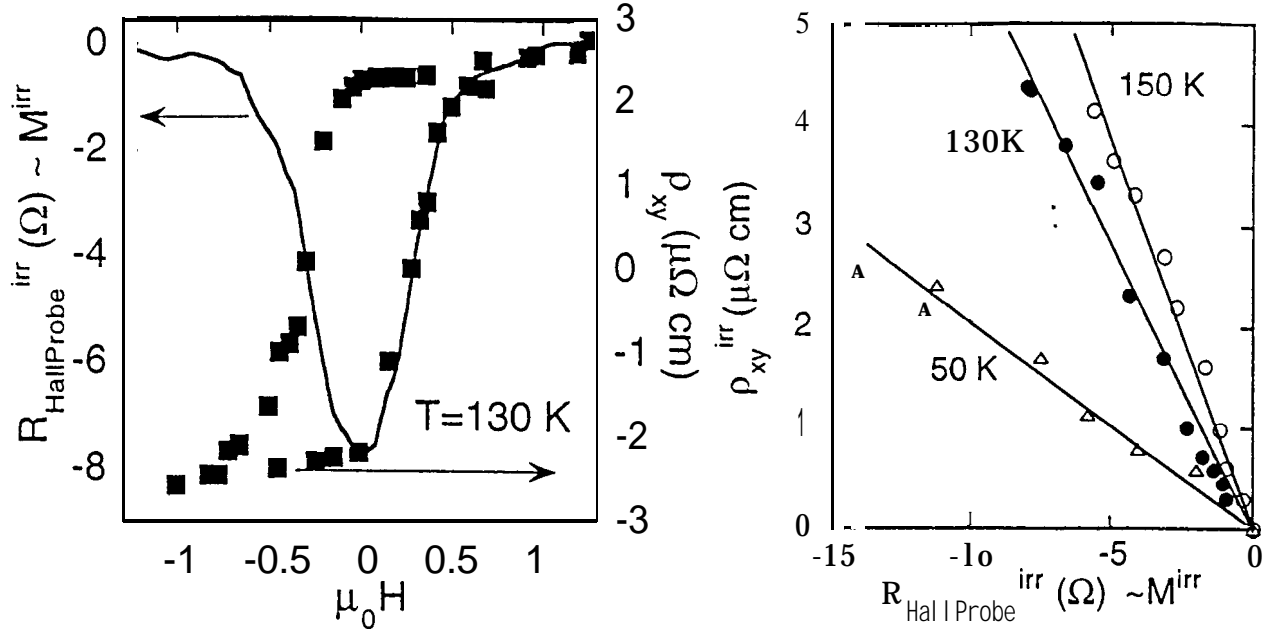


Fig. 2. Left panel: Plot of the irreversible part of the magnetization (left axis) and the Hall resistivity (right axis) versus field at $T=130$ K in the ceramics. Right panel: The irreversible part of the Hall resistivity as a function of the irreversible component of the magnetization for various temperatures below T_c . In both panels, the magnetization is measured using the Hall probe.

response of the system. Magnetic measurements are carried out in the ceramic samples by using the local Hall probe and SQUID magnetometers. The local Hall probe consists of an ion implanted GaAs sample with an active area of $\sim 100 \mu\text{m} \times 100 \mu\text{m}$. The Hall probe is placed directly on the top of the sample. The offset (longitudinal) resistance of the Hall probe is small (around 0.3Ω) and is subtracted from all the data. In the following, we will refer to the resistance of the Hall probe $R_{HallProbe}$ as the measured resistance minus this offset. At zero applied magnetic field, $R_{HallProbe}$ is directly proportional to the magnetization. However, the magnetization is small ($\mu_0 M < 0.2$ T), and at fields H larger than M , the signal in the probe, which senses the component of B perpendicular to its plane, is predominated by the applied magnetic field. Therefore, at large fields, we are only able to obtain the irreversible part of the magnetization M^{irr} which can be more easily extracted from the signal than the reversible component.

HALL EFFECT AND MAGNETIZATION DATA

First, we will demonstrate that the Hall resistivity is proportional to the magnetization. Shown in Fig. 2 (left panel) are ρ_{xy} (solid circles) and M^{irr} (solid line) versus magnetic field at $T=130$ K, in the ferromagnetic state. The Hall resistivity is hysteretic, and the form of the hysteretic loop is similar to that of the magnetization curve. The irreversibility in ρ_{xy} vanishes around 1 T at $T=130$ K, and so does M^{irr} at the same field. The right panel of Fig. 2 displays a linear dependence of the width of the hysteresis loop for the Hall resistivity ρ_{xy}^{irr} on M^{irr} . The linearity is checked for multiple temperatures below T_c .

With the SQUID measurements, we can verify the linearity between total ρ_{xy} and magnetization. An example is given in Fig. 3 for $T=200$ K. The Hall resistivity and magnetization scale perfectly with each other. The same is true for the data below T_c . That is, not only the hysteretic behavior of ρ_{xy} as a function of the applied magnetic field tracks that of the

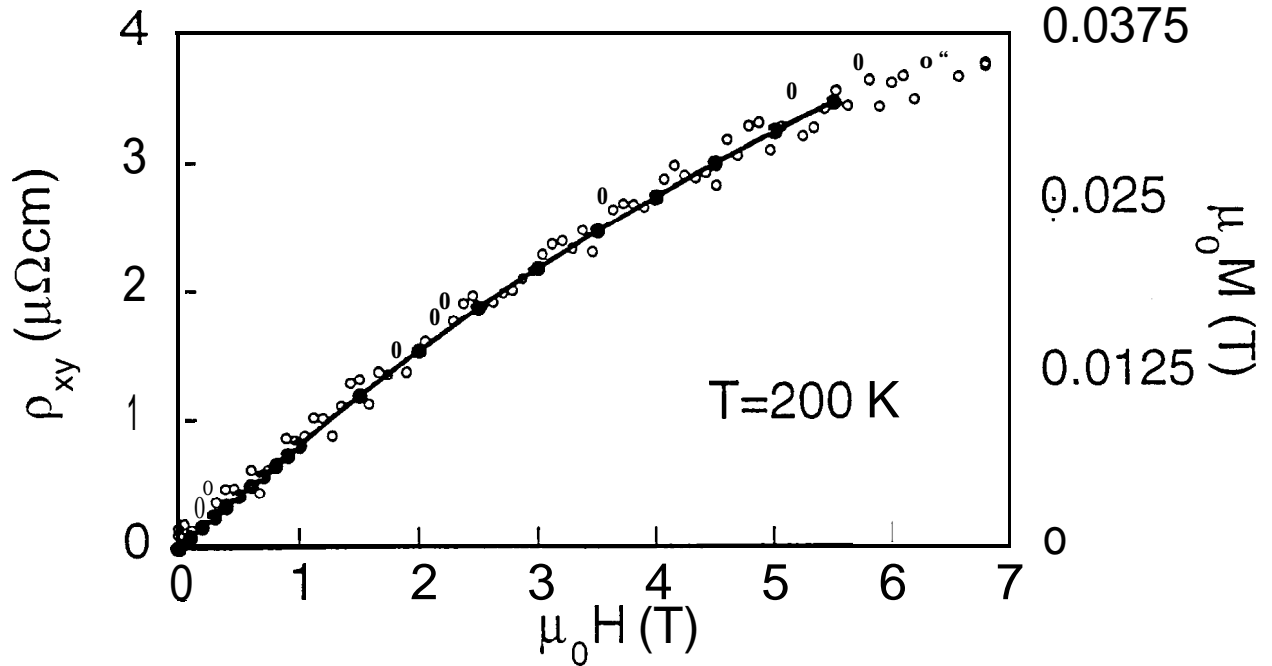


Fig. 3. The field dependence of ρ_{xy} and M at $T=200$ K. M is measured using the SQUID magnetometer.

magnetization, but also the field dependence of the Hall resistivity at high fields, in the reversible region, (see Fig. 4, central panel) mimics the magnetization behavior. From these data we conclude that the contribution from the normal Hall effect is negligible in comparison with the anomalous term.

Now we proceed to compare the Hall resistivity with the magnetoresistance (Fig. 4, left panel, data are taken at $T=150$ K). The longitudinal resistivity ρ decreases linearly with H at high fields and demonstrates a hysteretic behavior at low fields. In order to better show it, we subtract the linear term $\rho_{lin}(H)$ from the total resistivity ρ . The difference $\rho - \rho_{lin}$ is depicted in the central panel of Fig. 4. The maxima in $\rho - \rho_{lin}$ are very close to the fields at which the Hall resistivity (see Fig. 4, right panel) and magnetization take zero values at $T=150$ K, as shown by the arrows.

In the thin films, there is no hysteresis in either ρ or ρ_{xy} . In the ferromagnetic state, below $T_c \approx 180$ K, the initial linear rise of ρ_{xy} (Fig. 5) is followed by a second portion having a much smaller field gradient. As the temperature is increased above the Curie temperature, the deviation from the linear behavior becomes less pronounced and disappears for high enough temperatures in the entire magnetic field range (compare the isotherms at $T=195$ K and at $T=245$ K in Fig. 2, bottom). We assume that similarly to the case of the ceramic samples, the Hall resistivity in the films follows the magnetization and that the difference in the behaviors shown in Fig. 5, on the one hand, and Figs. 2-4, on another, is related to the difference in the $M(H)$ -dependences in films and ceramics.

From the data of Figs. 2-4 one can estimate the anomalous Hall coefficient R_s in the ceramic samples. $R_s(T)$ -dependence has a maximum near 200 K (detailed data will be published separately¹¹), with the peak value $\approx 1.1 \times 10^{-6} \text{ m}^3/\text{C}$. To estimate R_s in the thin films, we use the magnetization data obtained on fully oxygenated ceramic samples (in the low temperature limit, $\mu_0 M \approx 0.18 \text{ T}^{1.9}$). In the films, R_s is peaked at $T \approx 180$ K, with the

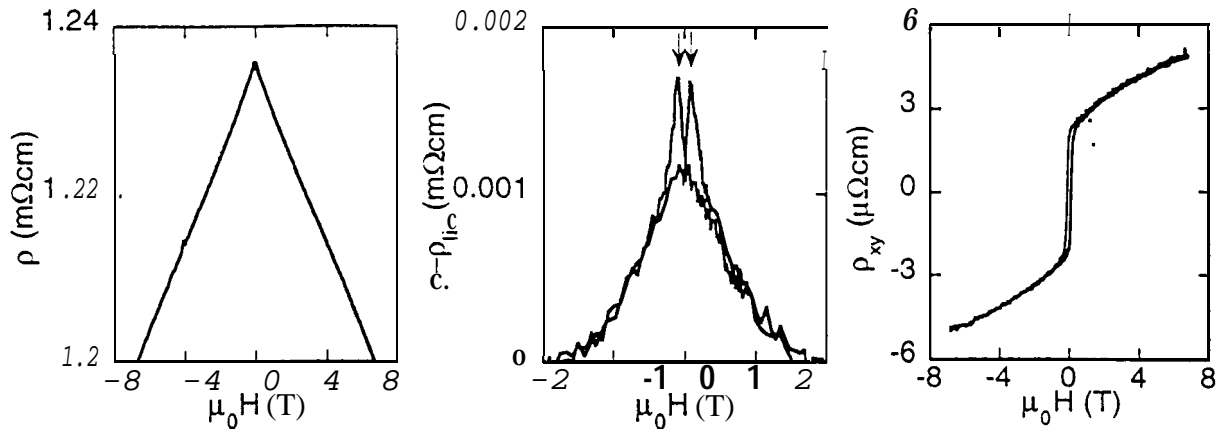


Fig. Left panel: The magnetoresistance of the ceramics at $T = 150$ K. Central panel: $\rho - \rho_{lin}$ (see the text) versus H at $T = 150$ K. Arrows show the fields at which M and ρ_{xy} are zero. Right panel: The field dependence of ρ_{xy} at $T = 150$ K in ceramics.

value $0.45 \times 10^{-6} \text{ m}^3/\text{C}$. In fact, the magnitude of the anomalous Hall coefficient observed in $\text{La}_{0.5}\text{Ca}_{0.5}\text{CoO}_3$ by far exceeds that for other ferromagnets^{1,11}. For instance, the R_s value in CoS_2 is $0.12 \times 10^{-6} \text{ m}^3/\text{C}$ ¹², in Fe $(0.5 \times 10^{-9}) \text{ m}^3/\text{C}$ ¹. Moreover, as we have discussed in Ref.¹¹, available theories of the Hall effect in ferromagnets^{3,4} predict seven orders of magnitude smaller values than in our experiment. One can speculate about the reasons why R_s in $\text{La}_{0.5}\text{Ca}_{0.5}\text{CoO}_3$ is larger than in other materials. Probably, the peculiar nature of magnetism in this compound caused by the existence of multiple spin configurations and the resulting enhancement of the spin fluctuations is responsible for this fact. What is difficult is to understand the reason for the enormous discrepancy between theory and experiment. Our results apparently call for strong theoretical efforts in this direction.

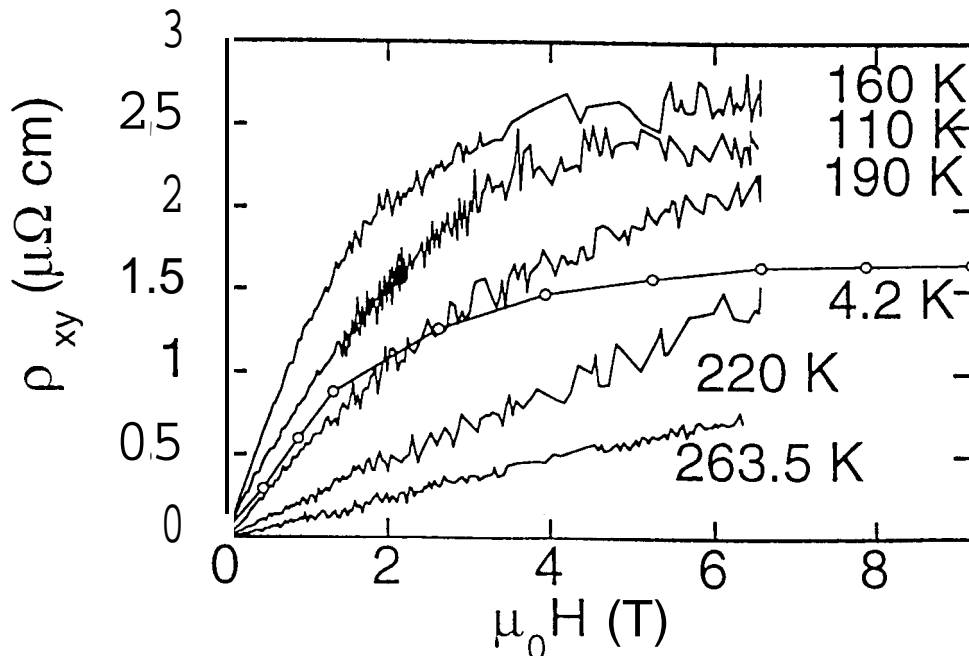


Fig. 5. The field dependence of ρ_{xy} in a thin film sample at various temperatures.

ACKNOWLEDGEMENTS

This work was jointly supported by NASA/OSS and the Caltech President's Fund. A. V. S. is a Millikan Senior Research Fellow in Physics.

REFERENCES

1. C. M. Hurd. The Hall effect in metals and alloys, Plenum Press. New York - London. 1972.
2. E. I. Kondorskii, A. V. Cheremushkina, and N. Kurbaniyazov, *Fizika Tverdogo Tela* **6**, 539 (1964) (*Soviet Physics -Solid State* **6**, 422 (1964)).
3. J. Kondo, *Prog. Theoret. Phys. (Japan)* **27**, 772 (1962).
4. F. E. Maranzana, *Phys. Rev. B* **160**, 421 (1967).
5. M. A. Señaris-Rodríguez and J. B. Goodenough, *J. Solid State Chem.* **118**, 323 (1995).
6. G. H. Jonker and J. H. van Santen. *Physics* **16**, 337 (1950).
7. C. Zener, *Phys. Rev.* **82**, 403 (1960).
8. P.-G. de Gennes, *Phys. Rev.* **118**, 141 (1960).
9. H. Taguchi, M. Shimada, and M. Koizumi, *J. Solid State Chem.* **41**, 329-332 [1982].
10. L. J. van der Pauw, *Philips Res. Reports* **13**, 1 (1958).
11. A. V. Samoilov, N. - C. Yeh, and R. P. Vasquez. preprint.
12. K. Adachi and K. Ohkohchi, *J. Phys. Soc. Jpn.* **49**, 154-161 (1980).